

Density estimation on low-dimensional manifolds: an inflation-deflation approach

Christian Horvat

*Department of Physiology
University of Bern
Bern, Switzerland*

CHRISTIAN.HORVAT@UNIBE.CH

Jean-Pascal Pfister

*Department of Physiology
University of Bern
Bern, Switzerland*

JEANPASCAL.PFISTER@UNIBE.CH

Abstract

Normalizing Flows (NFs) are universal density estimators based on Neuronal Networks. However, this universality is limited: the density's support needs to be diffeomorphic to a Euclidean space. In this paper, we propose a novel method to overcome this limitation without sacrificing universality. The proposed method inflates the data manifold by adding noise in the normal space, trains an NF on this inflated manifold, and, finally, deflates the learned density. Our main result provides sufficient conditions on the manifold and the specific choice of noise under which the corresponding estimator is exact. Our method has the same computational complexity as NFs and does not require computing an inverse flow. We also show that, if the embedding dimension is much larger than the manifold dimension, noise in the normal space can be well approximated by Gaussian noise. This allows to use our method for approximating arbitrary densities on non-flat manifolds provided that the manifold dimension is known.

Keywords: Normalizing Flow, Density Estimation, low-dimensional manifolds, normal space, noise

1. Introduction

Many modern problems involving high-dimensional data are formulated probabilistically. Key concepts, such as Bayesian Classification, Denoising, or Anomaly Detection, rely on the data generating density $p^*(x)$. Therefore, a main research area and of crucial importance is learning this data generating density $p^*(x)$ from samples.

For the case where the corresponding random variable $X \in \mathbb{R}^D$ takes values on a manifold diffeomorphic to \mathbb{R}^D , a Normalizing Flow (NF) can be used to learn $p^*(x)$ exactly (Huang et al. (2018)). However, in practice, many real-world applications such as predicting protein structures in molecular biology (Hamelryck et al. (2006)), learning motions in robotics (Feiten et al. (2013)), or predicting earthquake patterns in geology (Geller (1997)) are modeled on low-dimensional manifolds. Also, the manifold hypothesis states that high-dimensional datasets, such as high-resolution images, live closely on a low-dimensional manifold. Therefore, a few attempts have been made to use NFs to learn densities on low-dimensional manifolds, overcoming their topological constraint. To do so, these methods either need to know the manifold beforehand (Gemici et al. (2016), Rezende et al. (2020), Mathieu and Nickel (2020)), or sacrifice the directness of the estimate (Beitler et al. (2018), Kim et al. (2020), Cunningham et al. (2020), Brehmer and Cranmer (2020)).

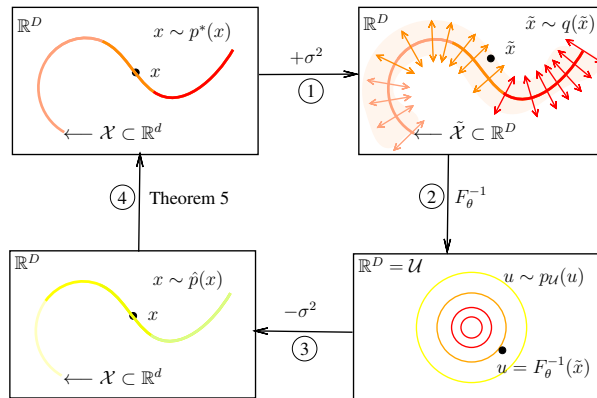


Figure 1: Schematic overview of our method. 1. A density $p^*(x)$ with support on a d -dimensional manifold \mathcal{X} (top left) is inflated by adding noise σ^2 in the normal space (top right). 2. We have an NF $F_\theta^{-1}(x)$ learn this inflated density $q(\tilde{x})$ using a well-known reference measure $p_U(u)$. 3. We deflate the learned density to obtain an estimate $\hat{p}(x)$ for $p^*(x)$. 4. Our main result provides sufficient conditions for the manifold \mathcal{X} and the choice of noise such that $\hat{p}(x) = p^*(x)$.

Our goal in this paper is to overcome both the aforementioned limitations of using NFs for density estimation on Riemannian manifolds. Given data points from a d -dimensional Riemannian manifold embedded in \mathbb{R}^D , $d < D$, we first inflate the manifold by adding a specific noise in the normal space direction of the manifold, then train an NF on this inflated manifold, and, finally, deflate the trained density by exploiting the choice of noise and the geometry of the manifold. See Figure 1 for a schematic overview of these points.

Our main theorem states sufficient conditions on the manifold and the type of noise we use for the inflation step such that the deflation becomes exact. To guarantee the exactness, we do need to know the manifold as in e.g. Rezende et al. (2020) because we need to be able to sample in the manifold’s normal space. However, as we will show, for the special case where $D \gg d$, the usual Gaussian noise is an excellent approximation for a noise in the normal space component. This allows to use our method for approximating arbitrary densities on Riemannian manifolds provided that the manifold dimension is known. In addition, our method is based on a single NF without the necessity to invert it. Hence, we don’t add any additional complexity to the training procedure of NFs. To the best of our knowledge, this is the first theoretical study that provides sufficient conditions for the learnability of a density with support on a low-dimensional manifold using NFs.

Notations: We denote the determinant of the Gram matrix of f as $g^f(x) := \det(J_f(x)^T J_f(x))$ where $J_f(x)$ is the Jacobian of f . We denote the Lebesgue measure in \mathbb{R}^n as λ_n . Random variables will be denoted with a capital letter, say X , and its corresponding state space with the calligraphic version, i.e. \mathcal{X} . Small letters correspond to vectors with dimensionality given by context. The letters d, D, n , and N are always natural numbers.

2. Background and problem statement

An NF transforms a known auxiliary random variable by using bijective mappings parametrized by Neuronal Networks such that the given data points are samples from this transformed random

variable, see Papamakarios et al. (2019) or Kobyzev et al. (2020) for some recent reviews. Formally, an NF is a diffeomorphism $F_\theta : \mathcal{U} \rightarrow \mathcal{X}$ and induces a density on \mathcal{X} through $p_\theta(x) = (g^{F_\theta}(u))^{-\frac{1}{2}} p_{\mathcal{U}}(u)$ where $p_{\mathcal{U}}(u)$ is known and $u = F_\theta^{-1}(x)$. The parameters θ are updated such that the KL-divergence between $p^*(x)$ and $p_\theta(x)$,

$$D_{KL}(p^*(x)||p_\theta(x)) = -\mathbb{E}_{x \sim p^*(x)}[\log p_\theta(x)] + \text{const.} \quad (1)$$

is minimized. If F_θ is expressive enough, it was proven that in the limit of infinitely many samples, updating θ to minimize this objective function converges to a θ^* such that it holds \mathbb{P}_X -almost surely $p^*(x) = p_{\theta^*}(x)$, see Huang et al. (2018).

More generally, let $X \in \mathcal{X} \subset \mathbb{R}^D$ be generated by an unobserved random variable $Z \in \mathcal{Z} \subset \mathbb{R}^d$ with density $\pi(z)$, that is $X = f(Z)$ for some function $f : \mathcal{Z} \rightarrow \mathcal{X}$ where typically $d < D$. If f is an embedding¹ (as it is the case in Gemici et al. (2016)) one can calculate probabilities such as $\mathbb{P}_X(A)$ for measurable $A \subset \mathcal{X}$ using a density $p^*(x)$ with respect to the volume form dV_f induced by f , that is

$$\mathbb{P}(X \in A) = \int_{f^{-1}(A)} \pi(z) dz = \int_A p^*(x) dV_f(x) \quad (2)$$

with $p^*(x) = \pi(z)g^f(z)^{-\frac{1}{2}}$ and $dV_f(x) = \sqrt{g^f(z)}dz$ where $z = f^{-1}(x)$. Hence, given an explicit mapping f and samples from $p^*(x)$, we can learn the unknown density $\pi(z)$ using a usual NF in \mathbb{R}^d . However, in general, the generating function f is either unknown or not an embedding creating numerical instabilities for training inputs close to singularity points.

In Brehmer and Cranmer (2020), f and the unknown density π are learned simultaneously. The main idea is to define f as a level set of a usual flow in \mathbb{R}^D and train it together with the flow in \mathbb{R}^d used to learn $\pi(z)$. To evaluate the density, one needs to invert f and thus this approach may be slow for high-dimensional data. Besides, to guarantee that f learns the manifold they proposed several ad hoc training strategies. We tie in with the idea to use an NF for learning $p^*(x)$ with unknown f and study the following problem.

Problem 1 *Let \mathcal{X} be a d -dimensional manifold embedded in \mathbb{R}^D . Let $X = f(Z)$ be a random variable generated by an embedding $f : \mathbb{R}^d \rightarrow \mathbb{R}^D$ and a random variable $Z \sim \pi(z)$ in \mathbb{R}^d . Given N samples from $p^*(x)$ as described above, find an estimator \hat{p} of p^* such that in the limit of infinitely many samples we have that $\hat{p}(x) = p^*(x)$, \mathbb{P}_X -almost surely.*

Remark 2

(i) *It is not obvious which reference measure to use for densities on manifolds (Pennec (2004)). This problem goes back to the Bertrand paradox for geometrical probabilities, see Chapter 1 in Kendall and Moran (1963). However, in our case, assuming that the random variable is generated by an embedding f_1 , the volume form dV_{f_1} is a natural choice. This is because dV_{f_1} is invariant under diffeomorphisms: if there is a diffeomorphism $\phi : \mathbb{R}^d \rightarrow \mathbb{R}^d$, such that $\sqrt{g^{f_2}(z)} = |\det \phi(z)| \cdot \sqrt{g^{f_1}(\phi(z))}$ where $f_2 = f_1 \circ \phi$, then $\int_A dV_{f_1} = \int_A dV_{f_2}$ for any measurable $A \subset \mathcal{X}$.² Hence, $p^*(x)$ is intrinsic to the manifold and does not depend on the specific embedding.*

1. Thus, a regular continuously differentiable mapping (called immersion) which is, restricted to its image, a homeomorphism.
 2. This follows immediately from the change of variable formula.

(ii) Viewing $p^*(x)dV_f$ as a differential d -form, we may say that the volume form dV_f is induced by the Euclidean metric in \mathbb{R}^D .

(iii) The concept of a density on a manifold can be generalized for orientable manifolds consisting of multiple charts. Also in this case, the volume form induced by the Euclidean metric is a natural choice.

3. Methods

To solve Problem 1, we want to exploit the universality of NFs. We want to inflate \mathcal{X} such that the inflated manifold $\tilde{\mathcal{X}}$ becomes diffeomorphic to a set \mathcal{U} on which a simple density exists. Doing so, allows us to learn the inflated density $q(\tilde{x})$ exactly using a single NF, see Section 2. Then, given such an estimator for the modified density, we approximate $p^*(x)$ and give sufficient conditions when this approximation is exact.

3.1 The Inflation step

Given a sample x of X , if we add some noise $\mathcal{E} \in \mathbb{R}^D$ to it, the resulting new random variable $\tilde{X} = X + \mathcal{E}$ has the following density

$$q(\tilde{x}) = \int_{\mathcal{X}} q(\tilde{x}|x)d\mathbb{P}_{\mathcal{X}}(x). \quad (3)$$

Denote the tangent space in x as T_x and the normal space as N_x . By definition, N_x is the orthogonal complement of T_x . Therefore, we can decompose the noise \mathcal{E} into its tangent and normal component, $\mathcal{E} = \mathcal{E}_t + \mathcal{E}_n$. In the following, we consider noise in the normal space only, i.e. $\mathcal{E}_t = 0$, and denote the density of the resulting random variable as $q_n(\tilde{x})$. The corresponding noise density $q_n(\tilde{x}|x)$ has mean x and domain N_x . We denote the support of $q_n(\cdot|x)$ by $N_{q_n(\cdot|x)}$. The random variable $\tilde{X} = X + \mathcal{E}_n$ is now defined on $\tilde{\mathcal{X}} = \bigcup_{x \in \mathcal{X}} N_{q_n(\cdot|x)}$. We want $\tilde{\mathcal{X}}$ to be diffeomorphic to a set \mathcal{U} on which a known density can be defined.

Example 1

(a) Let $\mathcal{X} = S^1 = \{x \in \mathbb{R}^2 \mid \|x\| = 1\}$ be the unit circle. For each $x \in S^1$ there exists $z \in [0, 2\pi)$ such that $x = e_r(x) = (\cos(z), \sin(z))^T$. To sample a point \tilde{x} in N_x , which is spanned by $e_r(x)$, we sample a scalar value γ and set $\tilde{x} = x + \gamma e_r(x)$. With $\Gamma \sim \text{Uniform}[-1, 1)$, we have that

$$\tilde{\mathcal{X}} = \bigcup_{x \in \mathcal{X}} \{x + \gamma e_r(x) \mid \gamma \in [-1, 1)\} = \{x \in \mathbb{R}^2 \mid \|x\|_2 < 2\} \quad (4)$$

which is the open disk with radius 2. The open disk is diffeomorphic to $(0, 1) \times (0, 1)$. Thus, $q_n(\tilde{x})$ can be learned by a single NF F^{-1} and $p_{\mathcal{U}}(u) = \text{Uniform}((0, 1) \times (0, 1))$ as reference.

(b) As in (a), we consider the unit circle. Now we set Γ to be a χ^2 -distribution with support $[-1, \infty)$. Then,

$$\tilde{\mathcal{X}} = \bigcup_{x \in \mathcal{X}} \{x + \gamma e_r(x) \mid \gamma \in [-1, \infty)\} = \mathbb{R}^2. \quad (5)$$

Thus, $q_n(\tilde{x})$ can be learned by a single NF F^{-1} and $p_{\mathcal{U}}(u) = \mathcal{N}(u; 0, I_D)$ as reference.

Both cases can be analogously extended to higher dimensions.

Remark 3

The random variable \mathcal{E}_n is generated by a random variable in \mathbb{R}^{D-d} , say Γ , with measure \mathbb{P}_Γ . Then, $q_n(\tilde{x}|x)$ is the density of the pushforward of the noise measure \mathbb{P}_Γ with regard to the mapping $h : \mathbb{R}^{D-d} \rightarrow N_x$. Hence, formally, the density $q(\tilde{x}|x)$ is with respect to the induced volume form dV_h , see Section 2. However, if we choose an orthonormal basis for N_x , say $n^{(1)}, \dots, n^{(D-d)}$, then we have that $\tilde{x} = x + h(\gamma) = x + A\gamma$ where the columns of $A \in \mathbb{R}^{D \times (D-d)}$ are given by these basis vectors, i.e. $A = [n^{(1)}, \dots, n^{(D-d)}]$. Thus, the Gram determinant of h is $g^h = \det(A^T A) = 1$ and we have that $dV_h(\tilde{x}) = d\gamma$ where $d\gamma$ denotes the volume form with respect to the $(D-d)$ -dimensional Lebesgue measure λ_{D-d} . In this sense, we can think of $q_n(\tilde{x}|x)$ as a density with respect to λ_{D-d} .

If, additionally, $q_n(\tilde{x}|x)$ depends only on $\|\tilde{x} - x\|$, as it is for the Gaussian distribution, we have that $q_n(\tilde{x}|x) = q_n(\|\tilde{x} - x\|) = q_n(\|\gamma\|)$ because h is an isomorphism. Thus, for this case it holds that $q_n(\tilde{x}|x)dV_h(\tilde{x}) = q_n(\|\gamma\|)d\gamma$. Then, for convenience, we may abuse notation by writing $\Gamma \sim q(\tilde{x}|x)$ or $\mathcal{E}_n \sim r(\gamma)$ where $r(\gamma)$ is the density of \mathbb{P}_Γ with respect to λ_{D-d} .

3.2 The Deflation step

Our main idea is to find conditions such that

$$q_n(\tilde{x}) = q_n(\tilde{x}|x)p^*(x) \tag{6}$$

for almost surely all $\tilde{x} \in \tilde{\mathcal{X}}$, and an almost surely unique $x \in \mathcal{X}$. Because then, given an exact estimator of $q_n(\tilde{x})$, say $\hat{q}_n(\tilde{x})$, we have for $\tilde{x} = x$ that $p^*(x) = \hat{q}_n(x)/q_n(x|x)$.

For equation (6) to be true, we need to guarantee that almost every \tilde{x} corresponds to only one $x \in \mathcal{X}$. This is certainly the case whenever all the normal spaces have no intersections at all (think of a simple line in \mathbb{R}^2). We can relax this assumption by allowing null-set intersections. Moreover, only those subsets of the normal spaces are of interest which are generated by the specific choice of noise $q_n(\tilde{x}|x)$. Thus, only the support of $q_n(\tilde{x}|x)$, $N_{q_n(\cdot|x)}$, matters. The key concept for our main result is expressed in the following definition:

Definition 4 Let \mathcal{X} be a d -dimensional manifold and N_x the normal space in $x \in \mathcal{X}$. Let $q_n(\cdot|x)$ be a density defined on N_x and denote by $N_{q_n(\cdot|x)}$ the domain of $q_n(\cdot|x)$. Denote the collection of all such densities as $Q := \{q_n(\cdot|x)\}_{x \in \mathcal{X}}$. For $\tilde{x} \in \tilde{\mathcal{X}}$, we define the set of all possible generators of \tilde{x} as $\mathcal{A}(\tilde{x}) = \{x' \in \mathcal{X} | N_{q_n(\cdot|x')} \ni \tilde{x}\}$. We say \mathcal{X} is Q -**normally reachable** if for all $x \in \mathcal{X}$, it holds that $\mathbb{P}_{\tilde{\mathcal{X}}|X=x}[\tilde{x} \in N_x | \#\mathcal{A}(\tilde{x}) > 1] = 0$ where $\#\mathcal{A}(\tilde{x})$ is the cardinality of the set $\mathcal{A}(\tilde{x})$. In words, every $\tilde{x} \in N_x$ is $\mathbb{P}_{\tilde{\mathcal{X}}|X=x}$ -almost surely determined by x .

To familiarize with this concept, consider Figure 2 and the following example:

Example 2 For the circle in example 1, we chose \mathcal{E}_n to be uniformly distributed on the half-open interval $[-1, 1)$. The point $(0, 0)^T$ is contained in $N_{q_n(\cdot|x)}$ for all $x \in \mathcal{X}$ and thus $N_{q_n(\cdot|x')} \cap N_{q_n(\cdot|x)} = \{(0, 0)^T\}$ for all $x \neq x'$, see Figure 2 (middle). Hence, for any given $\tilde{x} \in N_x$ we have that $\mathcal{A}(\tilde{x}) = \mathcal{X}$ if $\tilde{x} = (0, 0)^T$ and $\mathcal{A}(\tilde{x}) = x$ otherwise. Therefore, $\mathcal{A}(\tilde{x}) = \infty$ if $\tilde{x} = (0, 0)^T$ and $\mathcal{A}(\tilde{x}) = 1$ else.

Thus, $\mathbb{P}_{\tilde{X}|X=x} [\tilde{x} \in \tilde{\mathcal{X}} | \#\mathcal{A}(\tilde{x}) > 1] = \mathbb{P}_{\tilde{X}|X=x} [\tilde{x} = (0, 0)^T] = 0$ for all $x \in \mathcal{X}$. What follows is that \mathcal{X} is Q -normally reachable.

If we were to choose \mathcal{E}_n to be uniformly distributed on $[-1.5, 1]$, see Figure 2 (right), the normal spaces would overlap and we would have that $\mathbb{P}_{\tilde{X}|X=x} [\tilde{x} \in \tilde{\mathcal{X}} | \#\mathcal{A}(\tilde{x}) > 1] > 0$. In this case, \mathcal{X} would not be Q -normally reachable.

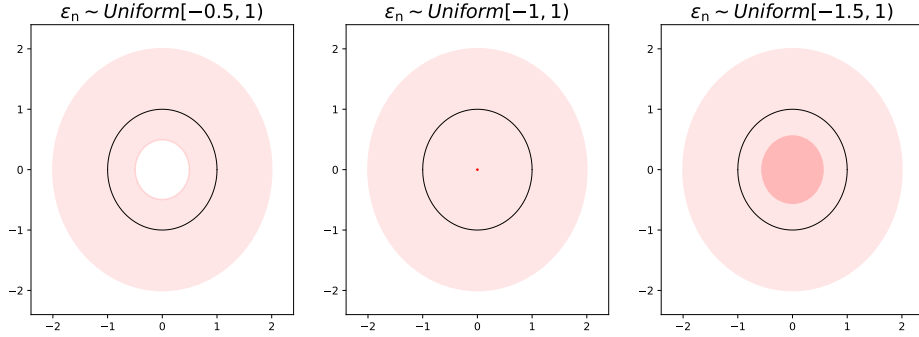


Figure 2: Q -normal reachability for different noise distributions $q_n(\tilde{x}|x)$ used to inflate $\mathcal{X} = S^1$ (black line). **Left:** \mathcal{X} is Q -normally reachable since every point in the inflated space $\tilde{\mathcal{X}}$ (red shaded area) has a unique generator. **Middle:** \mathcal{X} is Q -normally reachable since $\mathbb{P}_{\tilde{X}}$ -almost every point in $\tilde{\mathcal{X}}$ has a unique generator. **Right:** \mathcal{X} is not Q -normally reachable since every point in the dark shaded area has two generators.

Theorem 5 Let \mathcal{X} be a d -dimensional manifold. For each $x \in \mathcal{X}$, let $q_n(\cdot|x)$ denote a distribution on the normal space of x . Let \mathcal{X} be Q -normally reachable where $Q := \{q_n(\cdot|x)\}_{x \in \mathcal{X}}$. Assume that we can learn the density $q_n(\tilde{x})$ as defined in equation (3), by using a single NF F^{-1} , thus $q_n(\tilde{x}) = (g^F(F^{-1}(\tilde{x})))^{-\frac{1}{2}} p_{\mathcal{U}}(F^{-1}(\tilde{x}))$ for some known density $p_{\mathcal{U}}$. Then, for $\mathbb{P}_{\tilde{X}}$ -almost all $\tilde{x} \in \tilde{\mathcal{X}}$ holds that $q_n(\tilde{x}) = p^*(x)q_n(\tilde{x}|x)$, therefore, this equation, when evaluated at $\tilde{x} = x$, yields

$$p^*(x) = \frac{q_n(x)}{q_n(x|x)}. \quad (7)$$

The proof can be found in Appendix A.1.

3.3 Gaussian noise as normal noise and the choice of σ^2

Our proposed method depends on three critical points. First, we need to be able to sample in the normal space of \mathcal{X} . Second, we need to determine the magnitude and type of noise. Third, we need to make sure that the conditions of Theorem 5 are fulfilled. We address (partially) those three points.

1. For the special case where $D \gg d$, we show that a full Gaussian noise is an excellent approximation for a Gaussian noise restricted to the normal space. Consider $\mathcal{E} = \mathcal{E}_t + \mathcal{E}_n$, $\mathcal{E} \sim \mathcal{N}(0, \sigma^2 I_D)$. Then, the expected absolute squared error when approximating normal noise with full Gaussian

noise is $\mathbb{E}[|\mathcal{E} - \mathcal{E}_n|^2] = \mathbb{E}[|\mathcal{E}_t|^2] = d\sigma^2$. The expected relative squared error is therefore

$$\mathbb{E}\left[\frac{|\mathcal{E} - \mathcal{E}_n|^2}{|\mathcal{E}_n|^2}\right] = \mathbb{E}\left[\frac{|\mathcal{E}_t|^2}{|\mathcal{E}_n|^2}\right] = d\sigma^2 \mathbb{E}\left[\frac{1}{|\mathcal{E}_n|^2}\right] = \frac{d}{D-d-2} \quad (8)$$

because \mathcal{E}_t and \mathcal{E}_n are independent and $\frac{D-d}{|\mathcal{E}_n|^2}$ follows a scaled inverse χ^2 -distribution with $D-d$ degrees of freedom and scale parameter $1/\sigma^2$. Thus, if $D \gg d$, Gaussian noise is an excellent approximation for a Gaussian in the normal space. We denote the inflated density with Gaussian noise by $q_{\sigma^2}(\tilde{x})$ in the following.

More generally, it would be desirable to find constructive and scalable methods for sampling in the normal space. As a first approach, we propose a rejection based method in Section 5.1.1.

2. The inflation must not garble the manifold too much. For instance, adding Gaussian noise with magnitude $\sigma \geq r$ to S^1 will blur the circle. Since the curvature of the circle is $1/r$, intuitively, we want σ to scale with the second derivative of the generating function f . Additionally, we do not want to lose the information of $p^*(x)$ by inflating the manifold. If the generating distribution $\pi(z)$ makes a sharp transition at z_0 , $\pi(z_0 - \Delta z_0) \ll \pi(z_0 + \Delta z_0)$ for $|\Delta z_0| \ll 1$, adding too much noise in $x_0 = f(z_0)$ will smooth out that transition. Hence, we want σ to inversely scale with $\pi''(z)$. We formalize these intuitions in Proposition 6 and prove it in Appendix A.2. In accordance with Theorem 5, we say that $p_{\sigma^2}(\tilde{x})$ approximates well $p^*(x)$ if $\lim_{\sigma^2 \rightarrow 0} p_{\sigma^2}(x)/q_n(x|x) = p^*(x)$ for all $x \in \mathcal{X}$ where $q_n(x|x)$ is the normalization constant of a $(D-d)$ -dimensional Gaussian distribution.

Proposition 6 *Let $X \in \mathbb{R}^D$ be generated by $Z \sim \pi(z)$ through an embedding $f : \mathbb{R}^d \rightarrow \mathbb{R}^D$, i.e. $f(Z) = X$. Let $\pi \in C^2(\mathbb{R}^d)$. For $q_{\sigma^2}(\tilde{x})$ to approximate well $p^*(x)$, in the sense that $\lim_{\sigma^2 \rightarrow 0} q_{\sigma^2}(x)/q_n(x|x) = p^*(x)$ for $x \in \mathcal{X}$, a necessary condition is that:*

$$\left| \frac{\sigma^2}{2\pi(z_0)} \|\pi''(z_0) \odot (J_f^T J_f)^{-1}\|_+ \right| \ll 1 \quad (9)$$

where $\|A\|_+ = \sum_{i,j=1}^d A_{ij}$ for $A \in \mathbb{R}^d \times \mathbb{R}^d$, and \odot denotes the elementwise product, and $(\pi''(z_0))_{ij} = \frac{\partial^2 \pi(z)}{\partial z_i \partial z_j} \Big|_{z=z_0}$ is the Hessian of π evaluated at $z_0 = f^{-1}(x)$.

Intuitively, a second necessary condition is that the noise magnitude should be much smaller than the radius of the curvature of the manifold which directly depends on the second-order derivatives of f . This can be illustrated in the following example:

Example 3 *For the circle, in \mathbb{R}^2 generated by $f(z) = (\cos(z), \sin(z))^T$ and a von Mises distribution $\pi(z) \propto \exp(\kappa \cos(z))$, we get that $\sigma^2 \ll \min\left(\left|\frac{2r^2}{\kappa(\kappa \sin^2(z) - \cos(z))}\right|, r^2\right)$ where the first condition comes from Proposition 6 and the second one comes from the curvature argument.*

Even though this bound may not be useful as such in practice when f and π are unknown, it can still be used if f and π are estimated locally with nearest neighbor statistics.

From a numerical perspective, inflating a manifold using Gaussian noise circumvents degeneracy problems when training a vanilla NF for low-dimensional manifolds. In particular, the flows Jacobian determinant becomes numerically unstable, see equation (1). This determinant is essentially a volume-changing factor for balls. From a sampling perspective, these volumes can be estimated

with the number of samples falling into the ball divided by the total number of points. Therefore, we suggest to lower bound σ with the average nearest neighbor obtained from the training set to make sure that these volumes are not empty and thus avoid numerical instabilities.

3. Intuitively, if the curvature of the manifold is not too high and if the manifold is not too entangled, Q -normal reachability is satisfied for a sufficiently small magnitude of noise. In the manifold learning literature, the entangling can be measured by the reach number. Informally, the reach number provides a necessary condition on the manifold such that it is learnable through samples, see Chapter 2.3 in Berenfeld and Hoffmann (2019). Formally, the reach number is the maximum distance $\tau_{\mathcal{X}}$ such that for all \tilde{x} in a $\tau_{\mathcal{X}}$ -neighborhood of \mathcal{X} , the projection onto \mathcal{X} is unique. In Appendix A.3 we prove Theorem 7 which states that any closed manifold \mathcal{X} with $\tau_{\mathcal{X}} > 0$ is Q -normally reachable.

Theorem 7 *Let $\mathcal{X} \subset \mathbb{R}^D$ be a closed d -dimensional manifold. If \mathcal{X} has a positive reach number $\tau_{\mathcal{X}}$, then \mathcal{X} is Q -normally reachable where $Q := \{q_n(\cdot|x)\}_{x \in \mathcal{X}}$ is the collection of uniform distributions on a ball with radius $\tau_{\mathcal{X}}$, i.e. $q_n(\tilde{x}|x) = \text{Uniform}(\tilde{x}; B(x, \tau_{\mathcal{X}}) \cap N_x)$ where $B(x, \tau_{\mathcal{X}})$ denotes the D -dimensional ball with radius $\tau_{\mathcal{X}}$ and center x .*

To appreciate Theorem 7, we refer to the Tubular Neighborhood theorem, which states that every smooth and compact manifold has positive reach (see e.g. Lee (2019) for a proof).

4. Related work

Here, we give an overview of methods based on NFs for density estimation on low dimensional manifolds. One direction of research concentrates on densities defined on a given manifold, such as spheres or tori (Rezende and Mohamed, 2015, Rezende et al., 2020, Mathieu and Nickel, 2020). Orthogonal to that direction, Brehmer and Cranmer, 2020, Beitler et al., 2018, Kim et al., 2020, Cunningham et al., 2020 do not rely on an explicit chart while focusing on improving the generative ability. From the latter works, only Brehmer and Cranmer (2020) learn, in theory, the density on the manifold $p^*(x)$ exactly.

Cunningham et al., 2020 assume that data live on a noisy, i.e. inflated manifold and propose to learn a stochastic inverse $q(z|\tilde{x})$ of the generator $q(\tilde{x}|z)$. To train the parameters of $q(\tilde{x}|z)$, they rely on variational inference making this approach a special case of a Variational Auto Encoder. Their injective noisy flow improves the sampling quality compared to a baseline NF and, in addition, learns a latent representation. However, by construction, they only learn the inflated distribution $q(\tilde{x})$.

Kim et al., 2020 follow our methodology closely by inflating the manifold so that a usual NF can be used to learn the inflated density. For each sample x , they first draw a value c uniformly on $[0, 0.1]$, and then add a sample ν from $\mathcal{N}(0, c^2 I_D)$ to x , i.e. $\tilde{x} = x + \nu$. They learn the conditional distribution of the inflated manifold, $q(\tilde{x}|c)$, allowing for sampling on the manifold by setting $c = 0$. Their method does not require any knowledge of the manifold (neither the chart, nor the dimensionality), and improve 3D point cloud generation. However, they don't provide a deflation of the inflated distribution, and thus don't learn $p^*(x)$ exactly.

Beitler et al., 2018 propose to use different reference measures for the flow to encode the relevant manifold and irrelevant off-manifold directions. They propose to model the first d latent variables, say u , of the flow as standard Gaussian and the remaining $D - d$ variables, say v , as a diagonal

Gaussian with small variance. The hope is that maximum likelihood training is sufficient to encode the manifold in the first d components, so that a sampling procedure where the remaining $D - d$ components are set to 0, i.e. $v = 0$, would produce samples on the manifold. The gist is very similar to our idea expressed in equation (6). However, in general, this does not lead to the right density on the manifold, as explained in a footnote on page 4 in Brehmer and Cranmer, 2020, which justifies the name Pseudo-invertible encoder (PIE). Nevertheless, as noted by Brehmer and Cranmer, 2020, it is surprising that "somehow in practice learning dynamics and the inductive bias of the model seem to couple in a way that favor an alignment of the level set $v = 0$ with the data manifold. Understanding these dynamics better would be an interesting research goal." Our work gives a theoretical explanation why the PIE-model favors that alignment: When adding noise with small magnitude to the dataset (e.g. dequantization for images), the resulting density can be well approximated by a product of $p^*(x)$ and the noise distribution $q(\tilde{x}|x)$, see equation (6), such that treating the latent variables u and v differently, and thus having a product of two different measures as reference measure, biases the flow to learn this product form. A further interesting future direction would be to make this bias more explicit by constructing a flow for which the Jacobian determinant is in such a product form as well.

In Brehmer and Cranmer, 2020, the generating chart $f : \mathbb{R}^d \rightarrow \mathbb{R}^D$ is learned simultaneously with $p^*(x)$. They first transform x using a usual flow on \mathbb{R}^D , and then project to the first d components which is their proposal for f^{-1} . They then use another flow to learn the latent density π . To avoid calculating the Gram determinant of f , which is computationally expensive especially for $D \gg d$, they propose to train the parameters of f using the mean squared error while updating the parameters of π using maximum likelihood. They call the former manifold learning phase and the latter density learning phase. Different learning schemes (alternating and sequential) are proposed to ensure that f encodes the manifold and π captures the density. For the alternating scheme, they alternate for every epoch between a manifold training phase (updating the parameters of f), and the density training phase (updating the parameters for learning π). The experiments conducted by Brehmer and Cranmer, 2020 seem to verify that, indeed, $p^*(x)$ is learned exactly. Nevertheless, the ad-hoc training procedures without a unified maximum likelihood objective requires some further experimental verification.³

5. Results

We have three goals in this section: First, we numerically confirm the scaling factor in equation (7). Second, we verify that Gaussian noise can be used to approximate a Gaussian noise restricted to the normal space. Third, we numerically test our bound for σ^2 derived in Section 3.3. Finally, we show that we can learn complicated distributions on S^2 without using explicit charts. For training details, we refer to Appendix B.1 and B.3, respectively.

5.1 Von Mises on a circle

Let \mathcal{X} be a circle with radius 3 and let $\pi(z) \propto \exp(8 \cos(z))$ be a 1D von Mises distribution. Given $z \sim \pi(z)$, we generate a point in \mathcal{X} according to the mapping $f(z) = 3(\cos(z), \sin(z))$. We want to learn the induced density $p^*(x)$. Note that $3p^*(x) = \pi(z)$ since $1/3$ is the square root of the Gram determinant of f^{-1} . To benchmark our performance, we use the idea in Gemici et al. (2016)

3. We further motivate this requirement in Appendix B.4.

to first embed the circle into \mathbb{R} , using e.g. f^{-1} , learn the density there with an NF, and transform this learned density back to S^1 . In Brehmer and Cranmer (2020), this method is named Flow on manifolds (FOM) and we stick to this notation in the following. Note that f is not injective and to illustrate the benefit of our method we choose the singularity point to be $(1, 0)^T$. By moving points close to $(1, 0)^T$ slightly away from $(1, 0)^T$, we numerically ensure that f is an embedding.

1. The Inflation step: We inflate \mathcal{X} using 3 types of noise: Gaussian in the normal space (NG), Gaussian in the full ambient space (FG), and χ^2 -noise as described in examples 1(b) with scale parameter 3. Technically, NG violates the Q -normal reachability assumption. However, if σ^2 is small and the scale parameter for the von Mises distribution is large enough, this is practically fulfilled.

2. Learning $q_n(\tilde{x})$: For the NFs we use a Block Neural Autoregressive Flow (BNAF) (De Cao et al., 2020). We use the same NF architecture and training procedures across all models.

3. Deflation: Given an estimator for $q_n(\tilde{x})$, we use equation (7) to calculate $p^*(x)$. For FG and NG, we have that $q_n(x|x) = 1/\sqrt{2\pi\sigma^2}$ and for the normal χ^2 -noise is $q_n(x|x) = \sqrt{3}e^{-3/2}/(\sqrt{8}\Gamma(\frac{3}{2}))$.

In Figure 3, we show the results for $\sigma^2 = 0.01$ and $\sigma^2 = 1$. In the respective plot, the first row shows training samples from the inflated distributions $q_{\sigma^2}(\tilde{x})$ (left), and $q_n(\tilde{x})$ (middle), respectively. We color code a sample $\tilde{x} = x + \varepsilon$ according to $p^*(x)$ to illustrate the impact of noise on the inflated density. Note that the FOM model (top right) does not need any inflation and therefore is trained on samples from $p^*(x)$ only. In the respective plot, the second row shows the learned density for the different models and compares it to the ground truth von Mises distribution $\pi(z)$ depicted in black. As we can see, for $\sigma^2 = 0.01$ all models perform very well, although the FOM model slightly fails to capture $p(z)$ for z close to 0 which corresponds to the chosen singularity point. For $\sigma^2 = 1$, we see a significant drop in the performance of the Gaussian model. Although the manifold is significantly disturbed, the normal noise model still learns the density almost perfectly⁴, so does the normal χ^2 -noise model, as predicted by Theorem 5.

4. Note that our method still depends on how well an NF can learn the inflated distribution.

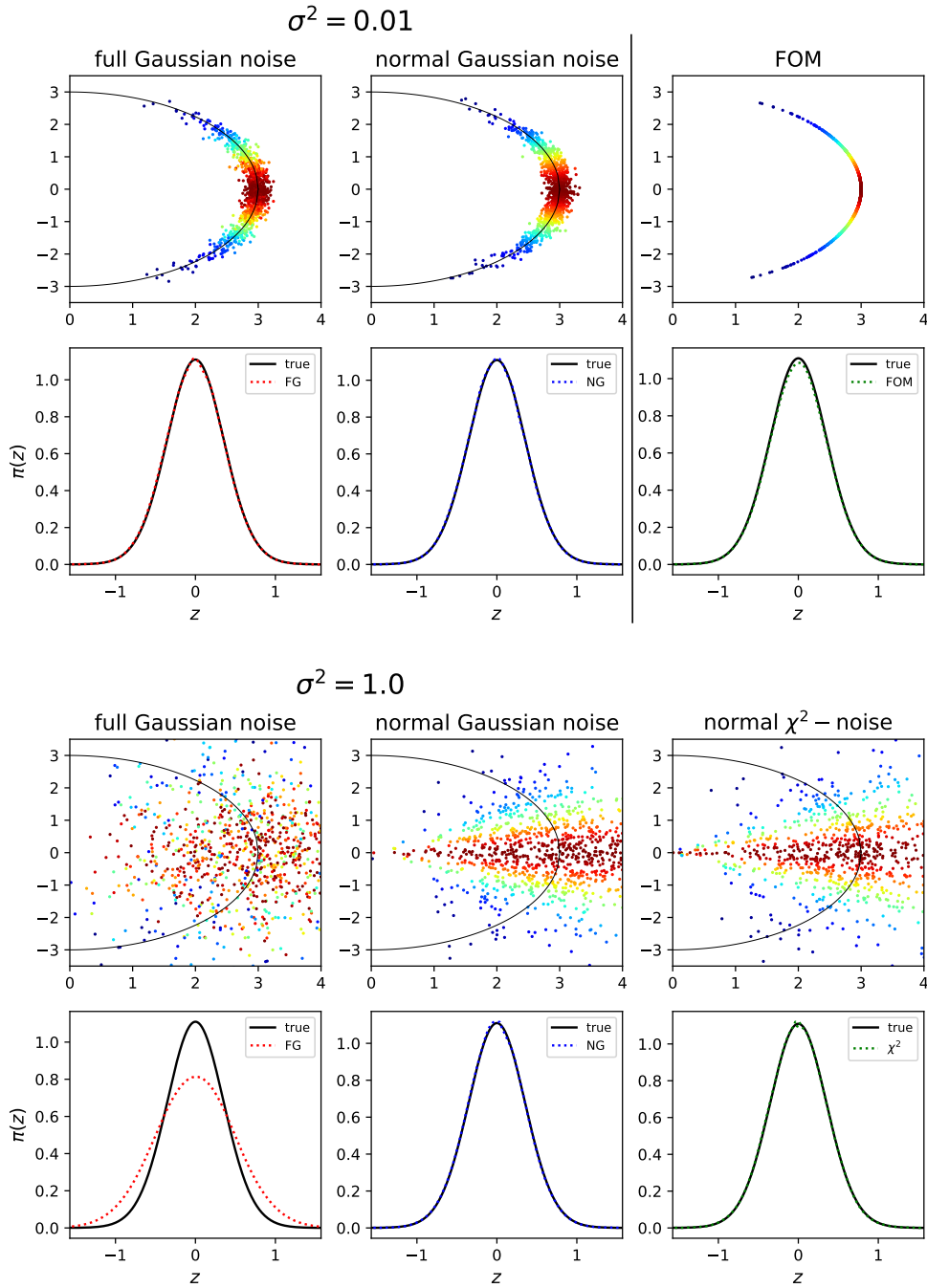


Figure 3: Learned densities for $\sigma^2 = 0.01$ (above) and $\sigma^2 = 1$ (below), respectively. **First row:** Samples used for training the respective model: FG (left), NG (middle), FOM/ χ^2 (right). The black line depicts the manifold \mathcal{X} (a circle with radius 3) and the colors code the value of $p^*(x)$. **Second row:** Colored line: Learned density $\hat{p}(x)$ according to equation (7) multiplied by 3. Blackline: ground truth von Mises distribution.

To measure the dependence of our method on the magnitude of noise, we iterate this experiment for various values of σ^2 and estimate the Kolmogorov-Smirnov (KS) statistics. The KS statistic is defined as $KS = \sup_{x \in \mathcal{X}} |F(x) - G(x)|$, where F and G are the cumulative distribution functions associated with the probability densities $p(x)$ and $q(x)$, respectively. By definition, $KS \in [0, 1]$ and $KS = 0$ if and only if $p(x) = q(x)$ for almost every $x \in \mathcal{X}$. However, equation (6) is only valid if the conditions of Theorem 5 are fulfilled. Note that the KS statistics is ill-posed in the case of full Gaussian noise since it doesn't lead to a density on the manifold \mathcal{X} . Nevertheless, we are interested in measuring the sensitivity to the noise, and thus consider the KS statistics as a relative performance measure.

In Figure 4, we display the KS values depending on different levels of noise, for the NG (blue) and FG (orange) noise compared with the ground truth von Mises distribution. Also, we embed the circle into higher dimensions $D = 5, 10, 15, 20$ and repeat this experiment. The result for $D = 2$ and $D = 20$ are shown in the first row (left and right).⁵ We add the performance of the FOM model (which is independent of σ^2) horizontally. Besides, we depict the lower and upper bound for σ^2 from Chapter 3.3 with dashed vertical lines. In the lower-left image, we show the optimal KS values obtained for both models depending on D . The lower-right image shows the corresponding σ^2 for those optimal KS . In bright, the optimal average σ^2 is shown whereas the dark regions are the minimum respectively maximum values for σ^2 such that we outperformed the FOM benchmark. We note that for both cases, the averaged optimal σ^2 is within the predicted bounds for σ^2 .

Several aspects are remarkable. The flat course of the KS vs. σ^2 plot is an indicator that the method is not very sensitive to noise and this does not change with the dimensionality of the embedding space. Also, the optimal KS values do not change much depending on D and the NS and FG model approach each other, as predicted.

Interestingly, the onset for the increase in the KS value for the NS-noise is roughly 3 which is the radius of the circle. For increasing σ^2 , $\tilde{\mathcal{X}}$ resembles more and more a double cone which is not diffeomorphic to \mathbb{R}^2 and thus the NF used to train the inflated distribution may not be able to capture the density close to the circle's center correctly. Also, the Q -normal reachability is more and more violated with an increasing σ^2 .

5.1.1 SAMPLING NOISE IN THE NORMAL SPACE

To generate samples close to the normal space, we propose to exploit our main theorem and the fact that the value of $q_n(\tilde{x})$ decays exponentially with the squared distance to the manifold when $q_n(\tilde{x}|x)$ depends on that distance. Then, for specific conditions, if we pre-train a model with some fixed σ^2 , $q_{\sigma^2}(\tilde{x})$, we can use it to generate standard Gaussian samples ε_n which are close to parallel to the normal space as follows, see Procedure 1.

See Figure 5 a) for a depiction of this intuition. If s^2 and the curvature of the manifold at x are small enough, the generating point x_k of $\tilde{x}_k = x + \varepsilon_k$, will be approximately in T_x . Then, the sample yielding the lowest log-likelihood is the one being the farthest away from the manifold, and hence it is the closest to the normal space of x .

We apply Procedure 1 the von Mises distribution on a circle studied before. A point $x + \varepsilon$ is in the normal space of N_x , if and only if the angle α between the directional vector ε and the normal space T_x is 0, see Figure 5 a). In Figure 5 b), we show how α is changing depending on the number of samples used with our procedure using a pre-trained model with $\sigma^2 = 0.00001$ and $s^2 = 0.5\sigma^2$.

5. Note that the scaling factor depends on D now, $q_n(x|x) = 1/(2\pi\sigma^2)^{\frac{D-d}{2}}$.

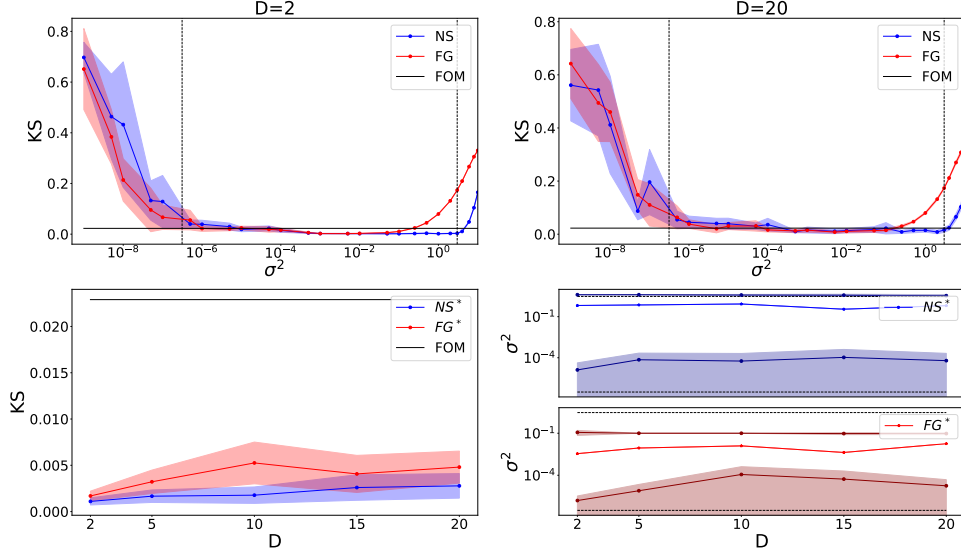


Figure 4: KS values for the NG- (**blue**) and FG-noise method (**orange**) depending on $\sigma^2 \in [10^{-9}, 10]$ and the embedding dimension $D = 5, 10, 15, 20$ in log-scale. For $D = 2$ (top left) and $D = 20$ (top right), the two vertical lines represent the lower and upper bound for σ^2 estimated according to Chapter 3.3 with 10K samples. We plot horizontally the KS value obtained from FOM. **Bottom left:** Optimal KS values depending on D . **Bottom right:** Optimal averaged σ^2 such that optimal KS is obtained (bright). The maximum and minimum σ^2 such that the FOM benchmark is outperformed (dark). The dashed horizontal lines are again the theoretical bounds. We used 10 seeds for the error bars and plot in log-scale.

Procedure 1 Generating Gaussian samples close to the normal space

Input: Pre-trained model q_{σ^2} , sample $x \sim p^*(x)$, scale parameter s^2

Output: Sample ε such that $\tilde{x} = x + \varepsilon$ is close in N_x

for $k = 1$ **to** K **do**

1. generate $\varepsilon_k \sim \mathcal{N}(0, I_D)$
2. normalize $\hat{\varepsilon}_k = \varepsilon_k / \|\varepsilon_k\|$
3. compute $\log q_{\sigma^2}(x + s^2 \hat{\varepsilon}_k)$

end for

\hookrightarrow get $k^* = \operatorname{argmin}_{k=1, \dots, K} \log q_{\sigma^2}(x + s \hat{\varepsilon}_k)$

\hookrightarrow set $\varepsilon = \varepsilon_{k^*}$

More precisely, we compute the expected distance using 100 samples of $p^*(x)$ with 10 additional trials for the error bars. We see that the expected angle α decays with the number of samples used across all dimensions. For $D = 20$ though, the method has only little effect on α because the samples are already very close to the normal space (as predicted in Section 3.3). For $D = 2$ in contrast, we can significantly decrease this distance. We have tried various values of s^2 , which is

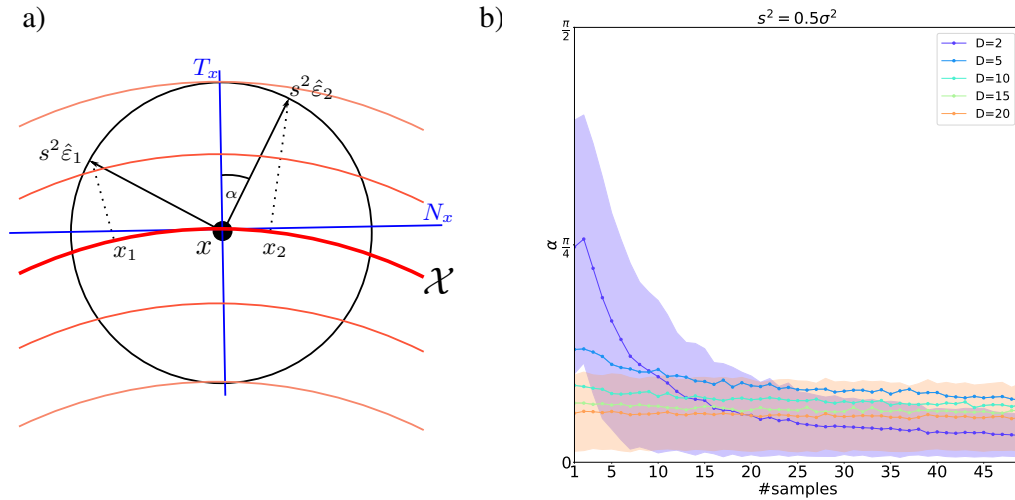


Figure 5: **a)** Intuition for generating normal space noise for $\mathcal{X} = S^1$. If x_1, x_2 are approximately in the tangent space T_x (blue line), where $p^*(x)$ is almost constant (red thick line), the $\hat{\varepsilon}$ with the greatest distance to the manifold will be the one closest to the normal space N_x in x since $q_{\sigma^2}(x + s^2 \hat{\varepsilon}_2) < q_{\sigma^2}(x + s^2 \hat{\varepsilon}_1)$ (fading red lines). **b)** Quality of normal space samples using the method described in Procedure 1 measured as the angle α to the normal space (the lower the better). We omit the error bars for the dimension 5, 10 and 15 to avoid clutter.

the radius of the sphere used to project the surrogate random variables ε onto, and found that it has no significant impact on the performance, see Appendix B.2 for more details.

5.2 Mixtures on S^2

We show that we can learn a complicated distribution, a mixture of 2-dimensional von Mises distributions on a sphere with radius 1, without using any knowledge about the manifold except for its intrinsic dimension. For certain magnitudes of σ^2 , we obtain similar estimates as the FOM benchmark as we can see in the direct comparison of the learned densities, see Figure 6 (top right), and the KS statistics⁶ (bottom right). As for the circle, the Gaussian restricted in the normal space allows for a greater range of noise magnitude without sacrificing the quality of the estimate.

6. Note that in 2D, the KS statistic needs to be modified as now the ordering matters. More concretely, comparing two random variables based on $\mathbb{P}(X_1 \leq x_1, X_2 \leq x_2)$ or based on $\mathbb{P}(X_1 \leq x_1, X_2 \geq x_2)$ (or any of the other two combinations) may lead to different results. Hence, for the KS value in 2D, we need to calculate the KS statistics based on all possible orderings and then take the maximum.

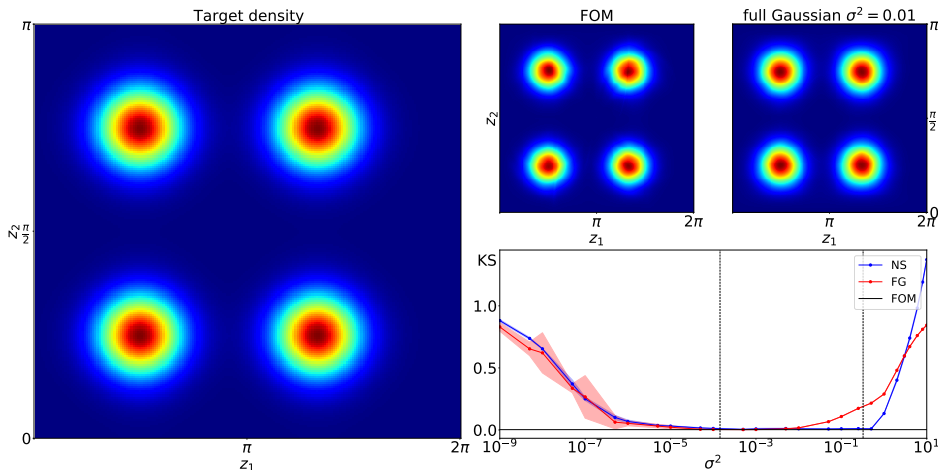


Figure 6: **Left:** Target density. **Upper right:** Learned densities using FOM and our method with Gaussian noise and $\sigma^2 = 0.01$. **Lower right:** KS vs. σ^2 plot of the Gaussian noise model (full and in normal space) compared to the FOM with the theoretical bounds from Chapter 3.3 for σ^2 depicted in vertical dashed lines (with 10K samples used to approximate these bounds).

6. Discussion

To overcome the limitations of NFs to learn a density $p^*(x)$ defined on a low-dimensional manifold, we proposed to embed the manifold into the ambient space such that it becomes diffeomorphic to \mathbb{R}^D , learn this inflated density using an NF, and, finally, deflate the inflated density according to Theorem 5. There, we provided sufficient conditions on the choice of inflation such that we can compute $p^*(x)$ exactly. Our method depends on some critical points which we addressed in Section 3.3. So far, the magnitude of noise σ^2 when using NFs on real-world data is somewhat chosen arbitrarily. As a step to overcome this arbitrariness, we derived an upper bound for σ^2 in Proposition 6 and established an interesting connection to the manifold learning literature in Theorem 7.

Our theoretical results open new research avenues. Using full Gaussian noise to learn the inflated distribution smears information on $p^*(x)$, in particular, if $p^*(x)$ has many local extrema. This loss of information may be especially impactful in out of distribution (OOD) detection or when it comes to adversarial robustness. Therefore, developing methods that allow generating noise in the manifold’s normal space could improve the performance of NFs on such tasks.

Another interesting direction is to exploit the product form of equation (6) and learn low-dimensional representations by forcing the NF to be noise insensitive in the first d -components and noise sensitive in the remaining ones. Inverting the corresponding flow allows sampling directly on the manifold.

Acknowledgments

We would like to thank Johann Brehmer for clarifying discussions on the manifold flow, and Simone C. Surace for useful discussions on manifolds.

This study has been supported by the Swiss National Science Foundation grant 31003A_175644.

Appendix A. Appendix

A.1 Proof of Theorem 5

We denote the probability measure of the random variable X as \mathbb{P}_X and it is defined on $(\mathcal{X}, \mathcal{B}(\mathcal{X}))$ where $\mathcal{B}(\mathcal{X})$ is the set of Borel sets in \mathbb{R}^D intersected with \mathcal{X} . For a realisation of X , say x , we denote the probability measure of the shifted random variable $x + \mathcal{E}_n$ as $\mathbb{P}_{\tilde{X}|X=x}$ and it is defined on $(\mathcal{N}_x, \mathcal{B}(\mathcal{N}_x))$. We extend both measures to $(\mathbb{R}^D, \mathcal{B}(\mathbb{R}^D))$ by setting the probabilities to 0 whenever a set $A \in \mathcal{B}(\mathbb{R}^D)$ has no intersection with \mathcal{X} or \mathcal{N}_x , respectively. For instance, that means for $\tilde{x} \in \mathcal{N}_x$ that

$$\mathbb{P}[x + \mathcal{E}_n \in (\tilde{x}, \tilde{x} + d\tilde{x})] = \mathbb{P}[x + \mathcal{E}_n \in (\tilde{x}, \tilde{x} + d\tilde{x}) \cap \mathcal{N}_x] = \mathbb{P}_{\tilde{X}|X=x}[(\tilde{x}, \tilde{x} + d\tilde{x}) \cap \mathcal{N}_x] \quad (10)$$

where $(\tilde{x}, \tilde{x} + d\tilde{x})$ denotes an infinitesimal volume element around \tilde{x} .

The mapping $(x, \varepsilon_n) \mapsto x + \varepsilon_n$ is $\mathcal{B}(\mathbb{R}^D) \times \mathcal{B}(\mathbb{R}^D)$ -measurable, and thus $\tilde{X} = X + \mathcal{E}_n$ is a random variable on $(\mathbb{R}^D, \mathcal{B}(\mathbb{R}^D))$ and has the pushforward of $\mathbb{P}_{(X, \varepsilon_n)}$ with regard to the mapping $(x, \varepsilon_n) \rightarrow x + \varepsilon_n$ as probability measure where $\mathbb{P}_{(X, \varepsilon_n)}$ is the joint measure of X and \mathcal{E}_n . Thus, for $A \in \mathcal{B}(\tilde{\mathcal{X}})$, we have that

$$\mathbb{P}_{\tilde{X}}(A) = \mathbb{P}_{(X, \varepsilon_n)}(\{(x, \varepsilon_n) \in \mathbb{R}^D \times \mathbb{R}^D | x + \varepsilon_n \in A\}). \quad (11)$$

Now let $\tilde{x} \in \mathcal{N}_x$ for an $x \in \mathcal{X}$. Since \mathcal{X} is Q -normally reachable, $\mathbb{P}_{\tilde{X}}$ -almost all \tilde{x} are uniquely determined by (x, ε_n) such that $\tilde{x} = x + \varepsilon_n$. Therefore, we have for $\mathbb{P}_{\tilde{X}}$ -almost all $\tilde{x} = x + \varepsilon_n$ that

$$\begin{aligned} \mathbb{P}_{\tilde{X}}((\tilde{x}, \tilde{x} + d\tilde{x}) \cap \tilde{\mathcal{X}}) &= \mathbb{P}_{(X, \varepsilon_n)}\left(\{(x, \varepsilon_n) \in \mathbb{R}^D \times \mathbb{R}^D | x + \varepsilon_n \in (\tilde{x}, \tilde{x} + d\tilde{x}) \cap \tilde{\mathcal{X}}\}\right) \\ &= \mathbb{P}\left(X + \mathcal{E}_n \in (\tilde{x}, \tilde{x} + d\tilde{x}) \cap \tilde{\mathcal{X}}\right) \\ &= \mathbb{P}(X \in (x, x + dx) \cap \mathcal{X}) \cdot \mathbb{P}(x + \mathcal{E}_n \in (\tilde{x}, \tilde{x} + d\tilde{x}) \cap \mathcal{N}_x) \\ &= \mathbb{P}_X((x, x + dx) \cap \mathcal{X}) \cdot \mathbb{P}_{\tilde{X}|X=x}((\tilde{x}, \tilde{x} + d\tilde{x}) \cap \mathcal{N}_x) \end{aligned} \quad (12)$$

where for the first equality we used equation (11) and for the third the fact that (x, ε_n) is almost surely uniquely determined by \tilde{x} .

Both probability measures on the right-hand side have a density. For \mathbb{P}_X with respect to dV_f , see Section 2, this density is $p^*(x)$. Similarly, since \mathcal{N}_x is a linear subspace of \mathbb{R}^D , $q_n(\tilde{x}|x)$ is the density of $\mathbb{P}_{\tilde{X}|X=x}$ with respect to the volume form dV_h where h is the mapping from \mathbb{R}^{D-d} to \mathcal{N}_x , see Remark 3. Then, the corresponding density of $\mathbb{P}_{\tilde{X}}$ is with respect to the measure $V := V_h \otimes V_f$. Therefore, we can write equation (12) in terms of densities as follows:

$$q_n(\tilde{x}) = p^*(x)q_n(\tilde{x}|x) \quad (13)$$

and it holds that

$$\begin{aligned} \int_{\tilde{\mathcal{X}}} q_n(\tilde{x}) dV(\tilde{x}) &= \int_{\mathcal{X}} \int_{N_x} p^*(x) q_n(\tilde{x}|x) dV_h(\tilde{x}) dV_f(x) \\ &= \int_{\mathcal{X}} p^*(x) dV_f(x) \\ &= 1, \end{aligned} \tag{14}$$

as needed for a density on $\tilde{\mathcal{X}}$. By setting \tilde{x} to x in equation (13), we obtain equation (7). Since we can learn $q_n(\tilde{x})$ exactly by assumption, this ends the proof.

Remark 8 (i) *The measure V is equivalent to λ_D when restricted to subsets of $\tilde{\mathcal{X}}$. This is because the column vectors of J_f and J_h form a basis of \mathbb{R}^D . These two measures are related as follows:*
 $\lambda_D(d\tilde{x}) = (g^f(x))^{-\frac{1}{2}} (g^h(\tilde{x}))^{-\frac{1}{2}} dV(\tilde{x})$.

(ii) *Note that in Theorem 5, we need that \tilde{X} is diffeomorphic to \mathbb{R}^D . This requires that the noise distribution $q_n(\cdot|x)$ is continuous for all x .*

A.2 Proof of Proposition 6

The generating function f is an embedding for \mathcal{X} and $X = f(Z)$ has the density $p^*(x)$ for $x \in \mathcal{X}$. We may extend the domain of $p^*(x)$ to include all points $x \in \mathbb{R}^D$ using the Dirac-delta function as follows

$$p^*(x) = \int_{\mathcal{Z}} \delta(x - f(z)) \pi(z) dz, \tag{15}$$

see Au and Tam (1999). After inflating X , we have that

$$p_{\Sigma}(\tilde{x}) = \int_{\mathcal{Z}} \mathcal{N}(\tilde{x}; f(z), \Sigma) \pi(z) dz \tag{16}$$

with covariance matrix $\Sigma \in \mathbb{R}^{D \times D}$. Assume $\tilde{x} = x$ for some $x \in \mathcal{X}$. We Taylor expand $f(x)$ around $z_0 = f^{-1}(x)$ up to first order,

$$f(z) \approx f(z_0) + J_f(z_0)(z - z_0), \tag{17}$$

and $\pi(z)$ up to second order,

$$\pi(z) \approx \pi(z_0) + \pi(z_0)'(z - z_0) + \frac{1}{2}(z - z_0)^T \pi''(z_0)(z - z_0). \tag{18}$$

where $\pi(z_0)'$ denotes the gradient and $\pi''(z_0)$ the Hessian of π evaluated at z_0 , thus $\pi(z_0)' \in \mathbb{R}^d$ and $\pi''(z_0) \in \mathbb{R}^{d \times d}$. Then, we can approximate $p_{\Sigma}(x)$ as follows:

$$\begin{aligned} p_{\Sigma}(x) &\approx \frac{1}{\sqrt{(2\pi)^D \det(\Sigma)}} \int_{\mathcal{Z}} \exp\left(-\frac{1}{2}(z - z_0)^T J_f^T \Sigma^{-1} J_f (z - z_0)\right) \\ &\quad \cdot (\pi(z_0) + \pi(z_0)'^T (z - z_0) + \frac{1}{2}(z - z_0)^T \pi''(z_0)(z - z_0)) dz. \end{aligned} \tag{19}$$

Now define $\hat{\Sigma}^{-1} = J_f^T \Sigma^{-1} J_f$. Then,

$$p_{\Sigma}(x) \approx \frac{\sqrt{\det(\hat{\Sigma})}}{\sqrt{(2\pi)^{D-d} \det(\Sigma)}} \int_{\mathcal{Z}} \frac{1}{\sqrt{(2\pi)^d \det(\hat{\Sigma})}} \exp\left(-\frac{1}{2}(z - z_0)^T \hat{\Sigma}^{-1} (z - z_0)\right) \cdot \left(\pi(z_0) + \pi(z_0)^T (z - z_0) + \frac{1}{2}(z - z_0)^T \pi''(z_0) (z - z_0)\right) dz. \quad (20)$$

Thus, we can exploit this Gaussian in \mathcal{Z} -space and get

$$\begin{aligned} p_{\Sigma}(x) &\approx \frac{\sqrt{\det(\hat{\Sigma})}}{\sqrt{\det(\Sigma)}} \left(\pi(z_0) + \frac{1}{2} \mathbb{E} [(z - z_0)^T \pi''(z_0) (z - z_0)]\right) \\ &= \frac{\sqrt{\det(\hat{\Sigma})}}{\sqrt{\det(\Sigma)}} \left(\pi(z_0) + \frac{1}{2} \|\pi''(z_0) \odot \hat{\Sigma}\|_+\right), \end{aligned} \quad (21)$$

where \odot stands for the elementwise multiplication and $\|A\|_+ = \sum_{i,j=1}^d A_{ij}$ for a $\mathbb{R}^d \times \mathbb{R}^d$ matrix A .

For the special case where $\Sigma = \sigma^2 I_D$, we can simplify this expression by exploiting that

$$\begin{aligned} \frac{\sqrt{\det(\hat{\Sigma})}}{\sqrt{(2\pi)^{D-d} \det(\Sigma)}} &= \frac{1}{(2\pi)^{\frac{D-d}{2}}} \frac{\sigma^{-D}}{\sigma^{-d} \sqrt{g^f}} \\ &= \frac{1}{(2\pi\sigma^2)^{\frac{D-d}{2}} \sqrt{g^f}}. \end{aligned} \quad (22)$$

Thus, in total, we get for this special choice of Σ

$$\begin{aligned} p_{\sigma^2}(x) &\approx \frac{1}{(2\pi\sigma^2)^{\frac{D-d}{2}} \sqrt{g^f}} \left(\pi(z_0) + \frac{\sigma^2}{2} \|\pi''(z_0) \odot (J_f^T J_f)^{-1}\|_+\right) \\ &= \frac{1}{(2\pi\sigma^2)^{\frac{D-d}{2}} \sqrt{g^f}} \pi(z_0) \left(1 + \frac{\sigma^2}{2\pi(z_0)} \|\pi''(z_0) \odot (J_f^T J_f)^{-1}\|_+\right) \end{aligned} \quad (23)$$

We assume now

$$\left| \frac{\sigma^2}{2\pi(z_0)} \|\pi''(z_0) \odot (J_f^T J_f)^{-1}\|_+ \right| \ll 1. \quad (24)$$

Note that $1/(2\pi\sigma^2)^{\frac{D-d}{2}}$ from equation (23) is exactly the normalization constant obtained when inflating the manifold with Gaussian noise in the normal space, $q_n(x|x) = 1/(2\pi\sigma^2)^{\frac{D-d}{2}}$. What follows is that $\lim_{\sigma^2 \rightarrow 0} p_{\sigma}(x)/q_n(x|x) = p^*(x)$ as we wanted to show.

A.3 Proof of Theorem 7

The theorem follows directly from the definition of the reach number $\tau_{\mathcal{X}}$ of \mathcal{X} . It is defined as the supremum of all $r \geq 0$ such that the orthogonal projection $\text{pr}_{\mathcal{X}}$ on \mathcal{X} is well-defined on the r -neighbourhood \mathcal{X}^r of \mathcal{X} ,

$$\mathcal{X}^r := \{\tilde{x} \in \mathbb{R}^D \mid \text{dist}(\tilde{x}, \mathcal{X}) \leq r\} \quad (25)$$

where $\text{dist}(\tilde{x}, \mathcal{X})$ denotes the distance of \tilde{x} to \mathcal{X} . Thus,

$$\tau_{\mathcal{X}} = \sup \{r \geq 0 \mid \forall \tilde{x} \in \mathbb{R}^D, \text{dist}(\tilde{x}, \mathcal{X}) \leq r \implies \exists! x \in \mathcal{X} \text{ s.t. } \text{dist}(\tilde{x}, \mathcal{X}) = \|\tilde{x} - x\|\}, \quad (26)$$

see Definition 2.1. in Berenfeld and Hoffmann (2019). By assumption $\tau_{\mathcal{X}} > 0$. Thus for all $\tilde{x} \in \mathcal{X}^{\tau_{\mathcal{X}}}$ we have that $x := \text{pr}_{\mathcal{X}}(\tilde{x})$ is unique. Since \mathcal{X} is a closed manifold, it must hold that $\tilde{x} \in N_x$ where N_x denotes the normal space in x . Let the noise generating distributions be a uniform distribution on the ball with radius $\tau_{\mathcal{X}}$, thus

$$q_n(\tilde{x}|x) = \text{Uniform}(\tilde{x}; B(x, \tau_{\mathcal{X}}) \cap N_x), \quad (27)$$

where $B(x, \tau_{\mathcal{X}})$ denotes a D -dimensional ball with radius $\tau_{\mathcal{X}}$ and center x . Then, we have for $\tilde{\mathcal{X}} = \bigcup_{x \in \mathcal{X}} N_{q_n(\cdot|x)}$ that

$$\tilde{\mathcal{X}} = \mathcal{X}^{\tau_{\mathcal{X}}}. \quad (28)$$

Thus, \mathcal{X} is Q -normally reachable where $Q := \{q_n(\cdot|x)\}_{x \in \mathcal{X}}$.

Appendix B. Experiments

B.1 Technical Details for circle experiments

For the Normalizing Flow $T^{-1}(x)$ we use a BNAF (Block Neural Autoregressive Flow) for the circle experiment. The number of hidden dimensions was adapted to the dimensionality of the data and the difficulty of the target density. These details are reported in the corresponding tabular. For the optimization scheme, we used Adam optimizer with an initial learning rate 0.1, a learning rate decay of 0.5 after 2000 optimization steps without improvement (learning rate patience). The batch size was set to 200. The total number of iterations (one iteration corresponds to updating the parameters using one batch sample) used is also reported in the tabular. No hyperparameter fine-tuning was done.

For the FOM and χ^2 -noise models, we use the same architecture as for the $D = 2$ case.

| Data dimension | hidden layers | hidden dimension | total parameters | iterations |
|----------------|---------------|------------------|------------------|------------|
| 2 | 3 | 100 | 31,204 | 70000 |
| 5 | 3 | 250 | 192,010 | 70000 |
| 10 | 3 | 500 | 764,000 | 70000 |
| 15 | 3 | 750 | 1,716,030 | 100000 |
| 20 | 3 | 1000 | 3,048,040 | 100000 |

Table 1: BNAF details for circle experiments.

B.2 Acceptance-Rejection method for normal noise generation

In Figure 7, we show how the quality of normal space samples depends on the free parameter s^2 . As we can see, the overall shape does not change significantly. As mentioned in the main text, for this procedure to work, we need σ^2 to be small - which is the case in Figure 7.

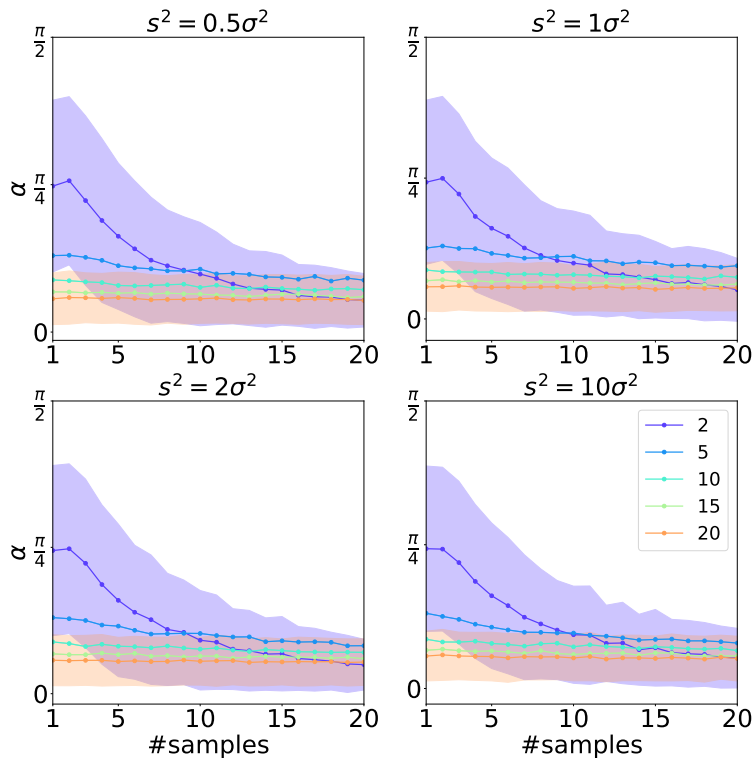


Figure 7: Quality of normal space samples using the method described in Procedure 1 measured as the angle α to the normal space (the lower the better) for various multiple of $\sigma^2 = 10^{-5}$ for s^2 . We omit the error bars for the dimension 5, 10 and 15 to avoid clutter.

B.3 Technical Details for the mixture of von Mises distributions on S^2

For the Normalizing Flow $T^{-1}(x)$ we use rational-quadratic neural spline flows, alternating coupling layers and random feature permutations, see Durkan et al. (2019). For the optimization scheme, we used AdamW (Loshchilov and Hutter (2017)) optimizer with an initial learning rate 0.0003, a learning rate cosine decay to 0 after every 2000 optimization steps, see Loshchilov and Hutter (2016), a weight decay of 0.0001 and a dropout probability of 0. The batch size was set to 200. No hyperparameter fine-tuning was done. See table 2 for more details. We use the same architecture for the FOM model and 3 seeds for the error bars.

| Coupling | residual blocks | hidden features | bins | spline range | total parameters | iterations |
|----------|-----------------|-----------------|------|--------------|------------------|------------|
| 10 | 3 | 50 | 8 | 3 | 171,845 | 50000 |

Table 2: BNAF details for a mixture of von Mises on S^2 .

The target distribution is a mixture of four von Mises distributions, $p_1^*(\phi_1, \theta_1), p_2^*(\phi_2, \theta_2), p_3^*(\phi_3, \theta_3)$ and $p_4^*(\phi_4, \theta_4)$. Each of those distributions has the same product form

$$p_i^*(\phi_i, \theta_i) = \frac{\exp(\kappa \cos(\theta_i - \mu_i))}{2\pi I_0(\kappa)} \cdot \frac{\exp(\kappa \cos(2(\phi_i - m_i)))}{\pi I_0(\kappa)}. \quad (29)$$

We set $\kappa = 6$. However, they differ in their mean values μ_i and m_i , see table 3. We used 3 different seeds in total to obtain the confidence intervals.

| i | μ_i | m_i |
|---|------------------|------------------|
| 1 | $\frac{\pi}{2}$ | $\frac{\pi}{4}$ |
| 2 | $\frac{4\pi}{3}$ | $\frac{3\pi}{4}$ |
| 3 | $\frac{\pi}{2}$ | $\frac{3\pi}{4}$ |
| 4 | $\frac{\pi}{4}$ | $\frac{4\pi}{3}$ |

Table 3: Mean values for the mixture of von Mises distributions.

B.4 Manifold Flow for the mixture of von Mises distributions on S^2

In this Subsection, we apply the manifold flow, see Section 4, on a mixture of von Mises distributions on a sphere, see Section 5.2. We do not attempt to find the optimal hyperparameters and training settings (such as batch- and training size, optimization method, or training scheduler) to maximize the performance.

The manifold flow (MF) proposed by Brehmer and Cranmer, 2020 uses two flows, one for encoding the data manifold to the latent space, and another for learning the latent density. To avoid calculating the Gram determinant of the encoding flow, they proposed different training procedures, an alternating, and a sequential (see Section 4 for more details). In Figure 8, we show that both methods learn the density reasonable good (top left and right). However, if we add Gaussian noise with magnitude 0.01 to the dataset, the two training schemes lead to very different results (bottom left and right). This illustrates the drawback of not having a unified maximum likelihood objective. We used the same model and training settings as for a similar dataset (a two-dimensional manifold embedded in \mathbb{R}^3) studied in Brehmer and Cranmer, 2020.

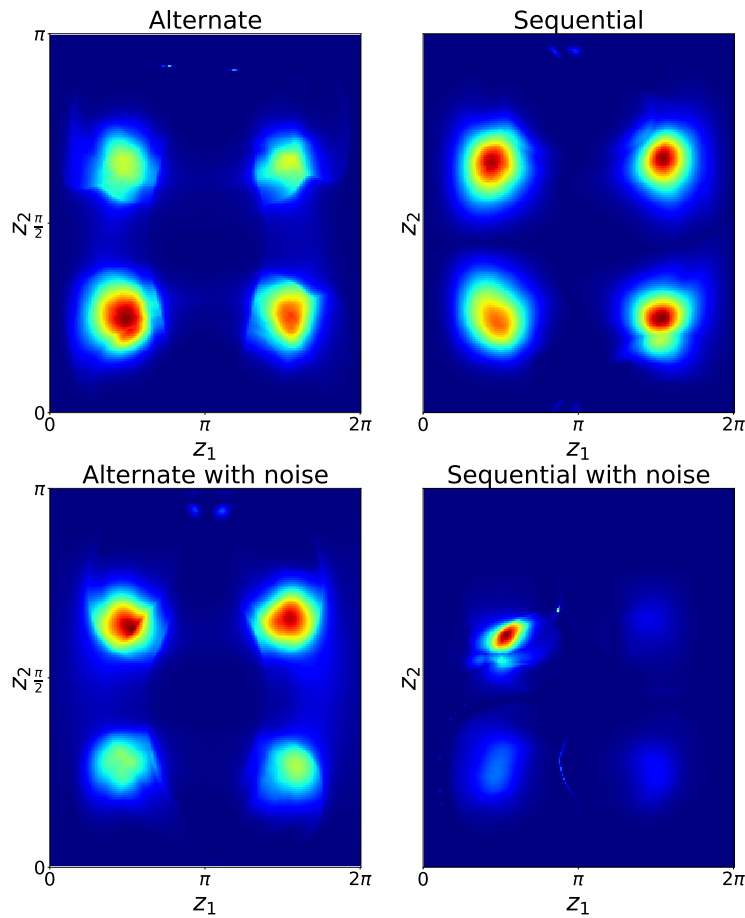


Figure 8: Performance of MF on the mixture of von Mises distributions on a sphere (top) and noisy sphere (bottom), using different training schemes (alternating left, and sequential right).

References

Chi Au and Judy Tam. Transforming variables using the dirac generalized function. *The American Statistician*, 53(3):270–272, 1999. doi: 10.1080/00031305.1999.10474472. URL <https://www.tandfonline.com/doi/abs/10.1080/00031305.1999.10474472>.

Jan Jetze Beitler, Ivan Sosnovik, and Arnold Smeulders. Pie: Pseudo-invertible encoder. 2018.

Clément Berenfeld and Marc Hoffmann. Density estimation on an unknown submanifold. *arXiv preprint arXiv:1910.08477*, 2019.

- Johann Brehmer and Kyle Cranmer. Flows for simultaneous manifold learning and density estimation. *Advances in Neural Information Processing Systems*, 33, 2020.
- Edmond Cunningham, Renos Zabounidis, Abhinav Agrawal, Ina Fiterau, and Daniel Sheldon. Normalizing flows across dimensions. *arXiv preprint arXiv:2006.13070*, 2020.
- Nicola De Cao, Wilker Aziz, and Ivan Titov. Block neural autoregressive flow. In *Uncertainty in Artificial Intelligence*, pages 1263–1273. PMLR, 2020.
- Conor Durkan, Artur Bekasov, Iain Murray, and George Papamakarios. Neural spline flows. In *Advances in Neural Information Processing Systems*, pages 7511–7522, 2019.
- Wendelin Feiten, Muriel Lang, and Sandra Hirche. Rigid motion estimation using mixtures of projected gaussians. In *Proceedings of the 16th International Conference on Information Fusion*, pages 1465–1472. IEEE, 2013.
- Robert J Geller. Earthquake prediction: a critical review. *Geophysical Journal International*, 131(3):425–450, 1997.
- Mevlana C Gemici, Danilo Rezende, and Shakir Mohamed. Normalizing flows on riemannian manifolds. *arXiv preprint arXiv:1611.02304*, 2016.
- Thomas Hamelryck, John T Kent, and Anders Krogh. Sampling realistic protein conformations using local structural bias. *PLoS Comput Biol*, 2(9):e131, 2006.
- Chin-Wei Huang, David Krueger, Alexandre Lacoste, and Aaron Courville. Neural autoregressive flows. volume 80 of *Proceedings of Machine Learning Research*, pages 2078–2087, Stockholm, Stockholm, Sweden, 10–15 Jul 2018. PMLR. URL <http://proceedings.mlr.press/v80/huang18d.html>.
- Maurice George Kendall and PAP Moran. *Geometric probability*. Griffin, 1963.
- Hyeongju Kim, Hyeonseung Lee, Woo Hyun Kang, Joun Yeop Lee, and Nam Soo Kim. Softflow: Probabilistic framework for normalizing flow on manifolds. *Advances in Neural Information Processing Systems*, 33, 2020.
- Ivan Kobyzev, Simon Prince, and Marcus Brubaker. Normalizing flows: An introduction and review of current methods. *IEEE Transactions on Pattern Analysis and Machine Intelligence*, 2020.
- J.M. Lee. *Introduction to Riemannian Manifolds*. Graduate Texts in Mathematics. Springer International Publishing, 2019. ISBN 9783319917542. URL <https://books.google.ch/books?id=UIPltQEACAAJ>.
- Ilya Loshchilov and Frank Hutter. Sgdr: Stochastic gradient descent with warm restarts. *arXiv preprint arXiv:1608.03983*, 2016.
- Ilya Loshchilov and Frank Hutter. Decoupled weight decay regularization. *arXiv preprint arXiv:1711.05101*, 2017.
- Emile Mathieu and Maximilian Nickel. Riemannian continuous normalizing flows. *arXiv preprint arXiv:2006.10605*, 2020.

George Papamakarios, Eric Nalisnick, Danilo Jimenez Rezende, Shakir Mohamed, and Balaji Lakshminarayanan. Normalizing flows for probabilistic modeling and inference. *arXiv preprint arXiv:1912.02762*, 2019.

Xavier Pennec. *Probabilities and statistics on riemannian manifolds: A geometric approach*. PhD thesis, INRIA, 2004.

Danilo Rezende and Shakir Mohamed. Variational inference with normalizing flows. In *International Conference on Machine Learning*, pages 1530–1538. PMLR, 2015.

Danilo Jimenez Rezende, George Papamakarios, Sébastien Racaniere, Michael Albergo, Gurtej Kanwar, Phiala Shanahan, and Kyle Cranmer. Normalizing flows on tori and spheres. In *International Conference on Machine Learning*, pages 8083–8092. PMLR, 2020.